

Advantages of operation flexibility and load sizing for PV-powered system design



Sterling Watson^a, David Bian^a, Nasim Sahraei^b, Amos G. Winter^{Va}, Tonio Buonassisi^{a,b}, Ian Marius Peters^{a,*}

^a Massachusetts Institute of Technology, United States

^b Singapore MIT Alliance for Research and Technology, Singapore

ARTICLE INFO

Keywords:

PV-powered systems
System design
Desalination

ABSTRACT

With their autonomous operation and low environmental impact, solar photovoltaics (PV) are an attractive power source for off-grid systems. However, the variable nature of solar energy is not well-suited to power conventional loads. Without careful consideration of the time-dependent power generation of PV, this discrepancy results in systems that are either over-designed and expensive, or compromise reliability. To accelerate the adoption of PV into new areas, it is essential to design PV-powered systems that are persistent, predictable, and affordable. In this paper, we analyze the cost reductions enabled by design optimization through time-flexible operation and improved load sizing. We consider two cases: (i) an idealized reference system, operating 8 h per day at 1 kW, generating an unspecified accumulable output, and (ii) a village-scale PV-powered electro-dialysis desalination system, designed to generate 10 m³ of drinking water per day. We found that time-flexible load operation reduced the power system cost of the idealized reference system by 39%, from \$2662 to \$1628, and designing its electrical load to operate for an optimal period of time enabled an additional cost reduction of 5% (to \$1503). For the village-based desalination system, we found that flexible operation paired with expected large decreases in membrane cost (from \$150 to \$20 per unit) reduced the associated power system cost by 57.6% from \$8935 to \$3788.

1. Introduction

Solar photovoltaics (PV) represent an autonomous and environmentally benign power source for off-grid systems. PV module prices have declined by a factor of 10 during the last decade, enabling their use in new markets (Haegel et al., 2017; pvinsights.com, 2017). However, adapting existing systems to PV power is not always straightforward. While conventional energy sources and grid electricity are dispatchable and non-variable, PV is naturally variable (Gowrisankaran et al., 2016). An electrical load designed to operate on a continuous conventional energy source requires adaptation to operate with a variable PV power source. A storage medium can buffer the variability of the PV power source, rendering solar power predictable and persistent (Bermudez, 2017; Nikolaidis et al., 2016). In this paper, we investigate the cost reductions enabled by time-flexible load operation and optimal load sizing in the design of a PV-powered system with energy and product storage.

A key challenge in the field of PV-powered systems is to create systems that are not only sufficiently non-variable, but also

simultaneously low-cost and reliable. Inadequate system design yields either excessive cost (over-design) or compromises reliability (under-design) (Glavin and Hurley, 2012). PV-powered systems installed in remote locations typically require both low cost and high reliability. Co-design (as opposed to independent, disaggregated design) of the PV subsystem, storage media, and electrical load represents an opportunity for cost reduction and technological innovation (Sahraei et al., 2017). Cost reductions through system optimization are essential to accelerate PV-powered system adoption in low-income, remote environments (Chaurey and Kandpal, 2010; Karakaya and Sriwannawit, 2015).

In this work, we demonstrate how time-flexible system operation—as opposed to continuous, non-variable operation—and load sizing can be implemented in off-grid PV powered systems, and how these strategies reduce the overall system cost by accommodating for the natural time-variance of available PV power (Denholm and Margolis, 2007). Here, the term “flexible operation” refers to process insensitivity to operating schedule, while “optimal load sizing” is the ability to scale the load power to approach the cost-optimum average operating time of the system. We demonstrate that systems, such as

* Corresponding author.

E-mail address: impeters@mit.edu (I.M. Peters).

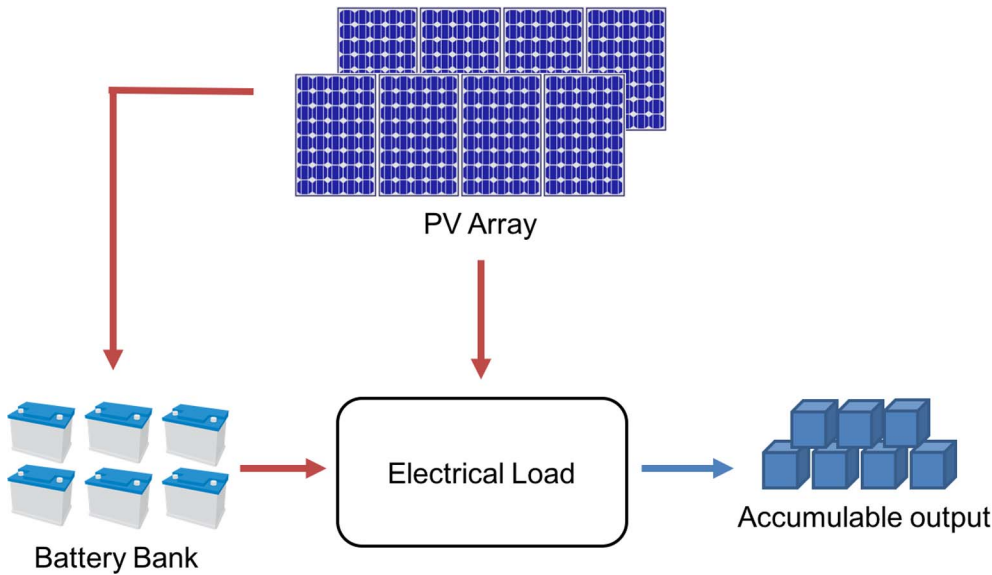


Fig. 1. The idealized reference system consisting of a 1 kW electrical load producing an accumulable output from 8 am to 4 pm daily; a PV array; and a battery bank. The PV array powers the load directly and charges the battery with excess power while the sun is shining. During times of low sunlight, the batteries power the load.

desalination or water pumping (EPRI, 2000), can accommodate some degree of time variance in operation without compromising critical performance by producing the correct amount of product averaged over a long amount of time, despite daily product variations. System cost is reduced by a decrease in the required storage capacity and PV array size. We also explore the cost reductions enabled by flexible load sizing—designing the load to operate at different power levels that complete the desired task over a corresponding duration, to accommodate for the diurnal and variable nature of solar energy.

We consider an idealized, reference system comprising a PV array, a battery bank, and a 1 kW electrical load producing an accumulable, storable output while operating 8 h per day from 8 am to 4 pm (Fig. 1). The PV array supplies power to the electrical load and the battery bank depending on the demands of each and the solar power available.

We then assess an actual prototype PV-powered electro dialysis reversal (PV-EDR) desalination system located near Hyderabad, India. We demonstrate how flexible operation and load sizing learnings can be incorporated into a system-design framework, to help accelerate the adoption of PV power across a wide range of applications. With a further adoption of PV, quality of life in remote areas can be improved, and the worst effects of climate change mitigated (Berney Needleman et al., 2016).

Previous work in the field of PV system optimization has focused on optimal power system sizing through simulation of electrical loads, power management, and PV power generation (Guo et al., 2015). Cost-optimized PV power systems for off-grid water pumping have been studied and tested, but have not analyzed the effects of flexible operation and load sizing (Olcán, 2015; Muhsen et al., 2016). Other work has focused on the optimization of off-grid reverse osmosis (RO) desalination systems powered by multiple energy sources (Bilton and Kelley, 2015; Habib et al., 2015). Sizing and scheduling multiple electrical loads in a microgrid setting to maximize solar energy utilization has also been studied (Habib et al., 2017; Jaramillo and Weidlich, 2016). The effect of temporal resolution on the sizing of an optimized PV-battery system has also been investigated previously (Beck et al., 2016).

2. Methods

2.1. Energy analysis

We used semi-empirical, satellite-based solar irradiance and temperature data from NSRDB (Renewable Energy Laboratory, 2016) for

the region of Chelluru, India, from 2014, the most recent year in which this data was available. This location was chosen because the PV-EDR case study system was constructed there. The calculations presented here used historical meteorological data for one year. Specifically, the meteorological data was used to establish the threshold for which the output generation in the system is turned on and off. While we do not expect this threshold to change much, time series spanning several years would help establishing variations in threshold or product output, and improve the predictability of the process. Furthermore, longer time series could help establish how the system is affected by a changing climate (for example, longer droughts). Alternatively, results could be compared to those obtained using a typical meteorological year (Bian et al., in preparation), provided that data is available.

The temperature-corrected efficiency of the solar panels at each time interval, η_{PV} , was calculated using (Brihmat and Mekhtoub, 2014),

$$\eta_{PV}(t) = \eta_{PV,nom} \cdot (1 + \alpha_p \cdot (T_{amb}(t) + k \cdot GHI(t) - T_{std})), \quad (1)$$

where $\eta_{PV,nom}$ is the nominal efficiency of the panels (15%), α_p is the temperature coefficient ($\alpha_p = -0.42\%$ Suniva Optimus Series Monocrystalline Solar Modules, 2016), $T_{amb}(t)$ is the ambient temperature, k is the Ross coefficient, which relates irradiance to module temperature ($k = 0.025$ Pearsall, 2017), $GHI(t)$ is the global horizontal irradiance, and T_{std} is the standard testing temperature (25 Celsius). The power produced by one square meter of solar panels, $P_{PV,1m}$, was calculated by multiplying the instantaneous PV efficiency, η_{PV} , by the instantaneous global horizontal irradiance $GHI(t)$. The PV array power output, P_{PV} , is simply the product of $P_{PV,1m}$ and the area of the PV array, A_{PV} .

The total energy stored in the battery bank E_{stored} was calculated via

$$E_{stored}(t) = E_{stored}(t-1) + t_{int} * \left(P_{PV}(t) - \frac{P_{load}(t)}{\eta_{conv}} \right) * \eta_{batt}, \quad (2)$$

during charging, and via

$$E_{stored}(t) = E_{stored}(t-1) - t_{int} * \left(\frac{P_{load}(t)}{\eta_{conv}} - P_{PV}(t) \right), \quad (3)$$

during discharging (Borowy and Salameh, 1996). Here, t_{int} is the interval length in seconds (300 s in this analysis), P_{PV} is the power being produced by the PV array, P_{load} is the power being consumed by the load, η_{conv} is the efficiency of the DC power converter (95%), and η_{batt} is the battery charge/discharge efficiency (85%) Linden and Reddy, 2002. Temperature effects were not considered in the battery operation because the battery banks for the reference and PV-EDR systems are

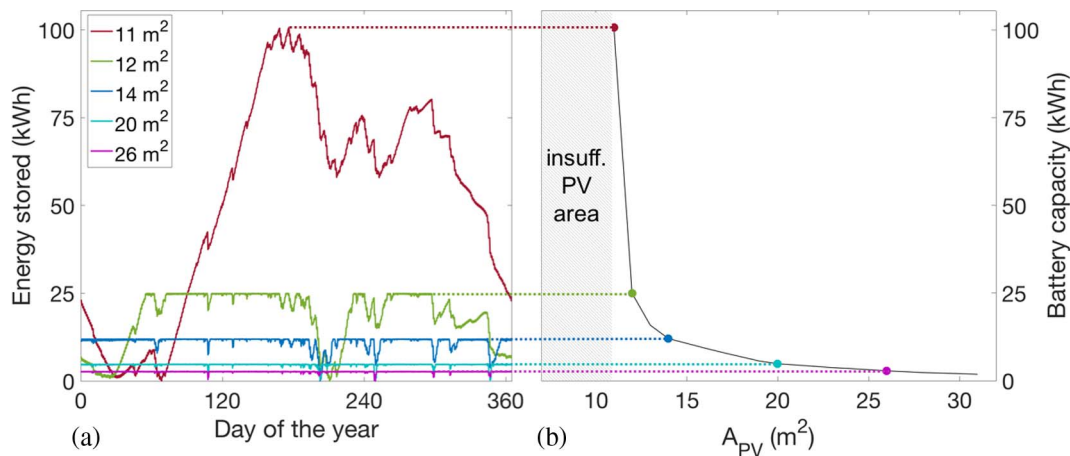


Fig. 2. (a) The energy stored in the battery of the reference system as a function of time for various areas of PV over the course of the reference year, calculated using NSRDB solar irradiance data for the Chelluru site in 2014; (b) the battery capacity requirement for each PV area. As PV area is increased beyond the minimum value (11 m²), battery storage is substituted by the PV panels, and the required capacity decreases. For areas below the minimum PV area (marked grey), the solar panels are not able to supply enough power for the system to run persistently throughout the year, no matter what the battery capacity is.

stored indoors, limiting the exposure to variations in operating temperature to close to ambient conditions.

The energy storage required for 100% output reliability was found by simulating the energy stored over the course of the entire reference year (Fig. 2). As the PV area is increased beyond a minimum value, the battery capacity required to buffer for intermittencies decreases (Borowy and Salameh, 1996). The minimum PV area is the area which, integrated over one year, delivers the total energy required in the same period. All points along the curve in Fig. 2(b) correspond to designs for which the 1 kW electrical load is powered for the designated time period (8 am to 4 pm) without fail. This condition shall be denoted as 100% output reliability. In recent literature (Chapman, 1987; Abouzahr and Ramakumar, 1991), a similar measure called “loss of power supply probability” (LPSP) was introduced, and defined as the average fraction of time that the load that is not supplied by the PV system. 100% output reliability corresponds to an LPSP of 0.

There is a minimum-cost combination of PV panels and batteries that can supply the 8-h, 1 kW fixed operating schedule reference system. This minimum-cost point lies somewhere on the curve shown in Fig. 2(b) and is made explicit in Fig. 3. Its value, indicated by the red ring in Fig. 3, depends on the ratio of the cost of batteries and the cost of PV. The costs of PV panels and lead acid batteries used here are \$98 per m² and \$150 per kWh, respectively. These values are representative for multicrystalline silicon PV panels and lead acid batteries (Shrikhande, 2016), and also reflect future cost targets for Li-ion batteries (Nykqvist and Nilsson, 2015). The U.S. Department of Energy, for example, states a goal to reduce the cost of batteries for electric vehicles to \$125/kWh by 2020 (Howell et al., 2016). The cost for multi-crystalline silicon solar panels has historically decreased by 24% each time cumulative production doubles (ISE, 2017). Compared to costs assumed here (65¢/Wp), prices are expected to drop to about half this value; the International Technology Roadmap for Photovoltaic (ITRPV) states 37¢/Wp for 2016 (E.e. International Technology Roadmap for Photovoltaic, 2017). The parallel lines in Fig. 3 represent constant power system cost for varying PV area and battery capacity combinations, and their slope is the ratio of energy storage cost per kWh to PV cost per square meter. If the cost ratio of energy storage to PV shifts, the slope of the iso-cost lines changes, as does the minimum value of any iso-cost line that intersects with the 100% output reliability curve. For example, if battery cost decreases relative to PV cost, the lines become steeper and the optimum cost shifts toward smaller solar panel areas (and vice versa).

¹ For interpretation of color in Fig. 3, the reader is referred to the web version of this article.

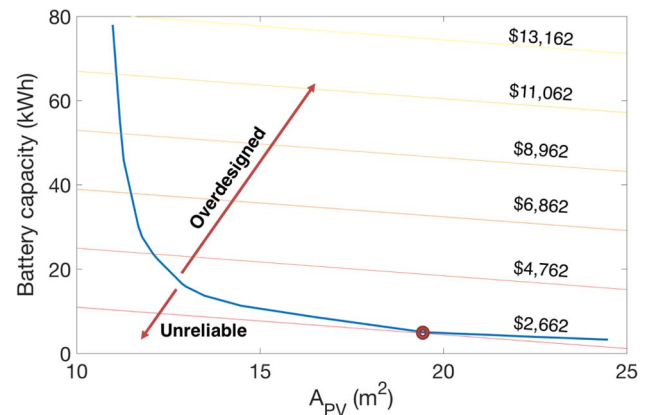


Fig. 3. Locus of power system designs (PV plus batteries) that can provide 100% output reliability in the reference year. To the right of the curve are overdesigned systems which provide excess power, and to the left of the curve are designs that do not provide adequate power or product over the course of the reference year. The diagonal lines represent iso-cost conditions for the power systems, and their slope is determined by the ratio of battery cost to PV panel cost. The intersection point on the locus of power system designs with the iso-cost curve of the lowest value corresponds to the lowest-cost power system (Borowy and Salameh, 1996).

The region above the 100% output reliability curve corresponds to overdesigned power systems which produce more than the required power output over the course of the reference year, and cost more than necessary. The region below the curve corresponds to systems with compromised reliability that will fail to produce the required power at some point during the year.

2.2. Product storage

For processes producing an accumulable output, storage of the output can serve as a secondary storage medium to batteries. Storage media can be substituted for one another if the load is operated on a flexible schedule. Matching production and solar energy available, and exploiting the possibility to substitute different storage media, can allow for system cost reductions under certain conditions.

In real scenarios, there may be a constraint on the amount of product or energy that can be stored at any given time. For example, there may not be enough space to allow for the cost-optimal quantity of product storage (as represented, for example, by a water tank). In such a scenario, the storage size would be limited in the optimization to a maximum value, and missing product storage would be compensated

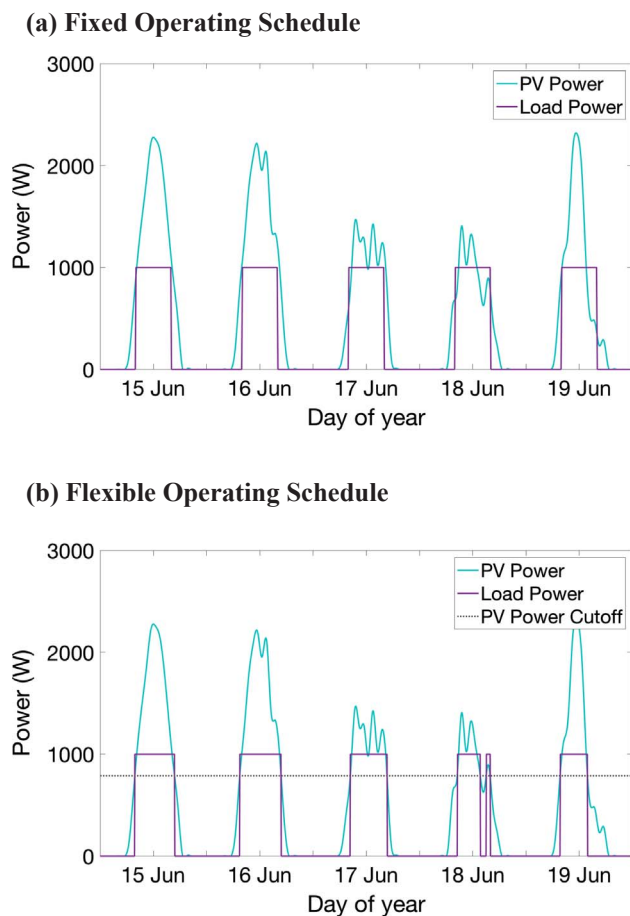


Fig. 4. (a) System with fixed operating schedule (8 am–4 pm at 1 kW) load power profile plotted against the power available from the solar power system over 5 days in June 2014; (b) system with flexible operating schedule (8 h daily average at 1 kW) load power profile and PV power cutoff beyond above which the load is turned on.

for with a larger energy storage unit. The resulting system would then have a higher cost than one at a site without space constraints.

3. Results

3.1. Flexible operation

In this section we investigate the power system cost reductions enabled by allowing the load operation schedule to shift in time for the 1 kW reference system. The operating schedule is determined depending on the instantaneous solar irradiance available, while an average operating time of 8 h per day is maintained. On long days with high solar irradiance, the system operates longer and stores the excess product to be collected on a day with low solar irradiance, such that the electrical load would not need to run at that time. We assume that product is collected at a constant rate throughout the year, i.e. 8 kWh worth of product is removed from the system every day.

The load profiles for the 1 kW reference PV power system for fixed and flexibly operated electrical loads, calculated using the 2014 Chelluru weather data, are shown in Fig. 4. The operation schedule that best matches the characteristic of solar irradiance for the location was determined by setting a cutoff irradiance value above which the load is turned on. The cutoff value was chosen such that the system runs on average for 8 h/day over the course of the reference year, and hence produces the same amount of product as a system operated for the same fixed 8-h daily schedule. For the flexible operation schedule, the frequency of number of hours operated per day for the reference year is presented in the histogram of Fig. 5. The spread shows the variability in

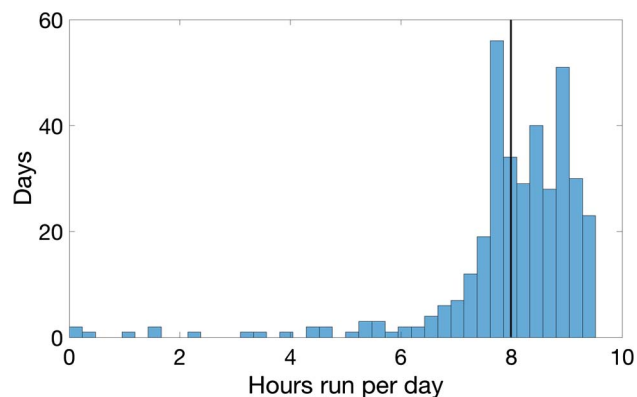


Fig. 5. Histogram of hours operated per day for the system under a flexible operation schedule. The average is 8 h, equivalent to the fixed operation schedule system. The spread shows the variability in days of abundant and scarce sunshine. Long operation of 8+ hours on some days of the year allows for short operation on the few days of the year for which there is very low PV power output.

days of abundant and scarce sunshine. Days with more than 8 h of operation allow producing a surplus that can be used during days with little solar energy available.

The flexible operation schedule improves the overlap of the load power and PV power profiles. The energy storage requirement associated with variable PV area for the 1 kW reference system operating flexibly for 8 h per day on average is shown in Fig. 6. For the same size PV array, the required energy storage is lower for the flexible operation case. This is shown in Fig. 6(a), with the flexible schedule battery capacity curve below the fixed schedule battery capacity curve for all PV array sizes. For example, at 14.5 m² of PV area, the required battery capacity is 11.4 kWh for the fixed operation system, and 1.7 kWh for the flexible operation system. Flexible operation also pushes the design toward a smaller PV array. The flexibly-operated design will also result in a variation of produced accumulative output over time. To guarantee that the specified amount of output is available every single day, excess production in days with long sun hours needs to be stored to provide for days with short sun hours. To provide 100% output reliability, 82 h worth of product would need to be stored to balance the fluctuations in annual solar availability in the presented example. 100% output reliability, is rarely required in realistic scenarios, however, and the amount of necessary storage is reduced significantly if the demand for output reliability is reduced. Furthermore, requirements for production may correlate with the availability of sunlight. For example, the demand for water desalination is greater on sunny days than on days with few sun hours, or even rain (Ji et al., 2010). Generally, flexible operation is cost-effective if the cost of product storage is smaller than the power system cost savings afforded by flexible operation—\$1034 in the case of the system considered here.

3.2. Optimal load sizing

Certain processes, such as drip irrigation and municipal water supply, require a roughly constant energy to produce a set output over a day, but the sizing of the unit and the power at which it operates can be flexible. For example, the pumping system for irrigation or a water tower could operate at a high flow rate for a shorter period of time, or a low flow rate for a longer period of time. Here, the flexibly-operated reference system operates on average 8 h per day, at 1 kW. Alternatively, a system of half the size could operate at 0.5 kW and produce the same output in 16 h. Or, another system twice the size of the original could operate at 2 kW and produce the desired output in 4 h. In each case, the energy used to run the system is the same, at an average of 8 kWh per day. There are various possibilities to realize the physical embodiment of such flexible operation. In some systems, the operating point can be adjusted; in other systems, the number of

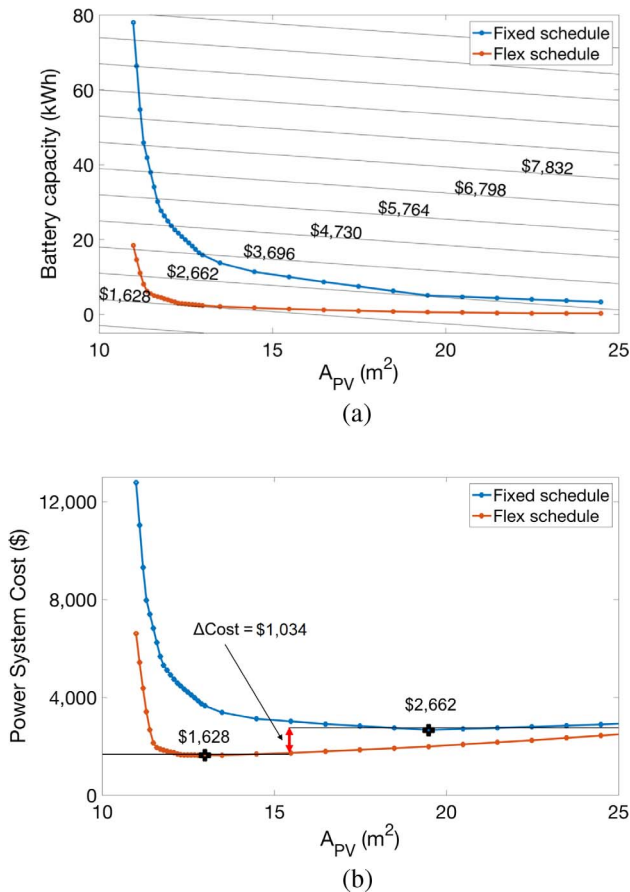


Fig. 6. (a) The relationship between PV array size and storage requirement (represented here as battery capacity) for the reference system operating according to fixed and flexible schedules. The diagonal lines represent lines of constant power system cost, increasing upwards, and are determined by the ratio of energy storage and PV cost. (b) The relationship between PV array size and total power system cost (PV + batteries) for both fixed and flexible schedule designs. The black markers indicate the points of lowest power system cost (\$2662 for fixed operation and \$1628 for flexible operation).

operating units can be scaled.

For systems using solar power, allowing flexibility in the duration of daily operation provides the possibility to reduce the power system cost by matching the length of operation to the number of available sun hours. The power system cost for designs with different lengths of average daily operating time but equivalent energy consumption per unit output are plotted in Fig. 7. The figure compares a fixed operating schedule (red) and a flexible operating schedule (blue) to illustrate under which general operating conditions a flexible operating schedule provides opportunities for cost reduction. To produce these results, the minimum power system cost was calculated for fixed and flexibly operated idealized PV-powered systems operating at each power level ranging from 2.67 kW (3 h average daily operation) to 0.47 kW (17 h average daily operation). More details about the calculation procedure are given in the [supporting material](#).

The flexible operating schedule provides the greatest cost reductions around an average daily operating time of 5–8 h, or corresponding power levels of 1.6 down to 1 kW. This enables a power system cost reduction of 43% from \$2662 to \$1503 compared to a fixed-schedule system. Note that these cost reductions only refer to the power system alone. Load sizing may also incur additional costs, as component costs may scale with load power for some applications. In such a case optimal electrical load sizing could push the average operating time to longer hours, when capital cost is considered. Flexible operation with load sizing is generally cost effective if the afforded cost reductions outweigh any additional costs that may occur for storage or operation – \$1159 in

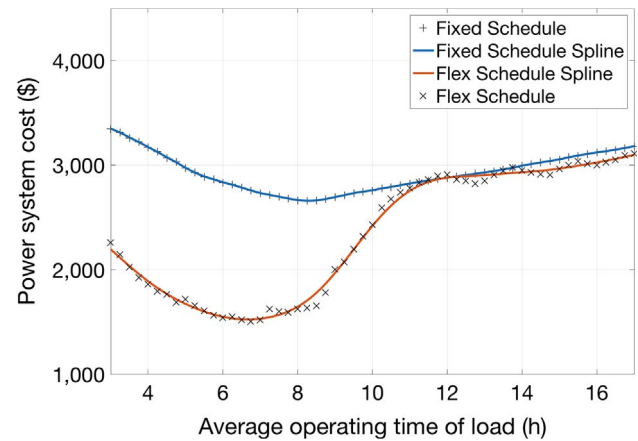


Fig. 7. Lowest-cost power system (PV plus batteries) for a flexibly-operated system (red line, x) with varying daily operating time/power levels and a system with fixed operating schedule (blue line, crosses). Lines are added as guides to the eye. Each design consumes an average of 8 kWh per day, but the power at which it operates and the corresponding number of hours it runs per day varies along the x-axis. The flexible-schedule systems have a lower cost than the fixed-schedule systems up to a 12-h daily operating time, at which point flexible operation does not provide value because the system must always run at some point when there is no sunshine available. (For interpretation of the references to color in this figure legend, the reader is referred to the web version of this article.)

this case.

3.3. Case study: PV-EDR system

A PV-powered electrodialysis reversal (PV-EDR) desalination system was designed and optimized for a village in rural India using a particle swarm optimization (PSO) (Fig. 8) (General Electric Water & Process Technologies, 2014). The system was required to provide 10,000 L of 300 mg/L desalinated drinking water per day, reliably throughout the year. The system was composed entirely of off-the-shelf components and a GE Model Number AQ3-1-2-50/35 EDR stack, for which the cost of a membrane cell pair is estimated \$150 according to supplier quotations (General Electric Water & Process Technologies, 2014).

Within the optimization (details in [Bian et al. \(in preparation\)](#)) design characteristics such as area of PV panels, quantity of batteries, and number of EDR membrane cell pairs were varied to find the lowest-cost PV-EDR system that could meet specified village drinking water requirements. For each design, the performance of the PV-EDR system over the reference year using the Chelluru solar irradiance and weather data from 2014 was calculated, ruling out infeasible designs such as those that violated the physics of EDR operation or those that did not produce the requisite quality and quantity of water. The EDR unit was designed to operate in batch mode, continuously recirculating a batch of water through the stack until the desired salinity was reached. In the simulation, the operating conditions were such that a batch should be run whenever there was sufficient charge in the batteries to complete a batch and enough space in the water storage tank to accommodate the desalinated water. These operation conditions formed an intrinsic flexibility in the schedule by which the system was run. Through iteration, the optimization scheme converged to a design with a total capital cost of \$23,420 (Table 1).

Desalination rate is proportional to the number of EDR membrane cell pairs in the EDR unit. To produce 10,000 L per day, the optimized PV-EDR system had to operate for an average 17:42 h per day. Aside from several outliers, the system was expected to run 17:42 h per day (Fig. 9). The optimization converged on this design with a long operation schedule because it allowed for a smaller EDR unit, which is the largest contributor to capital cost. Because of the dominance of membrane cost, a flexible operation schedule for this PV-EDR system did not result in significant cost reductions of the power system compared to a

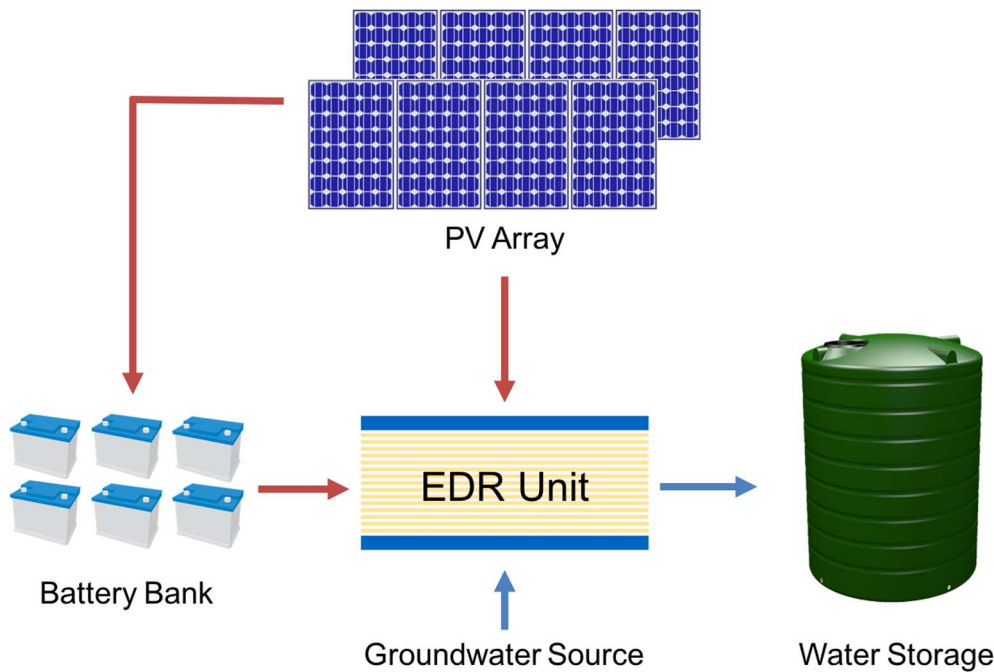


Fig. 8. Schematic of the PV-EDR system main components. The red lines represent energy flows, while the blue lines represent water flows. The size of the PV array, battery bank, water storage tank, and EDR desalination unit were all varied in the particle swarm optimization to determine the lowest-capital cost system, given current off-the-shelf component prices. (For interpretation of the references to color in this figure legend, the reader is referred to the web version of this article.)

Table 1
Cost and quantity of components in the optimized PV-EDR design. The total optimized system cost was \$23,420. Graphical information about the system and the design parameters is provided in the supporting material (compare Fig. S4).

Design variable	Symbol	Cost	Quantity
PV area	A_{PV}	\$98/m ²	57.5 m ²
Battery capacity	E_{batt}	\$150/kW h	22 kW h
Water storage volume	V_{bank}	\$110/m ³	10 m ³
No. of EDR cell pairs	N_{CP}	\$150/cell pair	62
No. of electrodes	N_{elec}	\$2000/electrode	2
Stack voltage	v_{EDR}	N/A	45 V
Batch size	V_{batch}	N/A	0.42 m ³
Daily operating time	t_{op}	N/A	17:42 h
Peak power	P_{pk}	N/A	1562 W

per cell pair equivalent (Hangzhou Iontech Environmental Technology Company Limited, 2014) is feasible today. Electrodialysis membranes are a small market right now and their cost is expected to drop further if economies of scale take effect. To investigate the impact of significant, but reasonable reductions in membrane cost, we performed the PV-EDR optimization using a membrane cell pair cost of \$20 (Bian et al., in preparation). The optimized PV-EDR design with this reduced membrane cost is summarized in Table 2, and has a daily operating time of 8:35 h, and hence, benefits from flexible operation. A comparison of the hours operated per day for the EDR systems optimized for \$150 and \$20 cell pairs is shown in Fig. 9. The \$20 cell pair design has a larger EDR stack enabled by the lower cost of membranes, and correspondingly shorter average operating time and higher peak power. Its power profile is better matched to the solar profile, allowing the PV array to downsize from 58 m² to 31 m², and the batteries to be downsized from 22 kW h to 5 kW h. This represents a power system cost reduction of \$5147, or 57.6%.

Results shown in Tables 1 and 2 and in Fig. 9 underline the advantages of designing an electrical load that can perform the required task in a time period during which sunlight is available, enabling a smaller PV array and battery bank. When the load is not required to run at night, flexibility in the operating schedule reduces the amount of time it needs to run in low-irradiance conditions.

Table 2
Cost and quantity of components in an optimized PV-EDR design, where membrane cost was reduced from \$150 to \$20 per cell pair. The total optimized system cost was \$11,717. This represents a power system cost reduction (PV and batteries) of 57.6% compared to the 17:42 h/day PV-EDR design. A detailed description of the system is found in the supporting material (compare Fig. S4).

Design variable	Symbol	Cost	Quantity
PV area	A_{PV}	\$98/m ²	31 m ²
Battery capacity	E_{batt}	\$150/kW h	5 kW h
Water storage volume	V_{bank}	\$110/m ³	10 m ³
No. of EDR cell pairs	N_{CP}	\$20/cell pair	133
No. of electrodes	N_{elec}	\$2000/electrode	2
Stack voltage	v_{EDR}	N/A	95 V
Batch size	V_{batch}	N/A	0.68 m ³
Daily operating time	t_{op}	N/A	8:35 h
Peak power	P_{pk}	N/A	2360 W

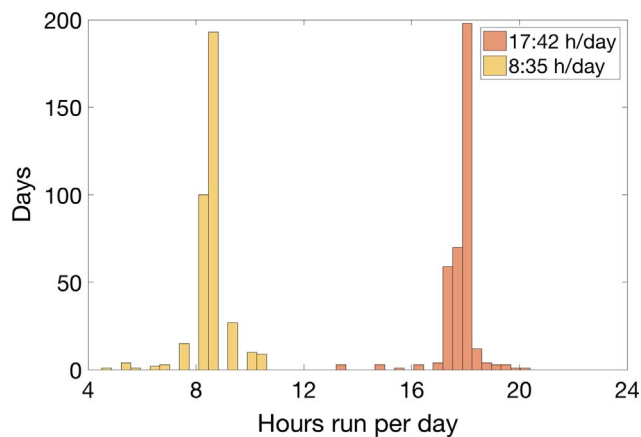


Fig. 9. Histograms of the EDR system designed to run on average 8:35 h/day (\$20 cell pairs) and 17:42 h/day (\$150 cell pairs). Note that both systems are operated flexibly. Considering the results from , cost reductions due to flexible operation are afforded by the system running 8:35 h/day.

fixed schedule.

However, it is not unreasonable to assume that membrane costs will drop significantly. According to manufacturer quotations from Iontech, a company producing electrodialysis systems, a membrane cost of \$40

4. Discussion

4.1. Generalization of presented results

We used specific examples in this paper to illustrate how time-flexible operation and load sizing is used to reduce the cost for PV-powered stand-alone systems. Specific input in our calculations was the cost for PV and batteries (\$98/m² and \$150/kWh), as well as the location for which the meteorological data was obtained (Hyderabad, India). We also used specific numbers for the load power, as different load power scales linearly with the resulting PV areas and battery capacities. Changing cost for PV and batteries will affect the composition of the PV power system. As pointed out in Fig. 3, the ratio of the two costs determines which composition is the most cost-effective; the lowest cost point is determined by the tangent of the straight line with a slope given by the cost ratio. We expect the cost for both PV panels and batteries to further decline in the future. Depending on which technology has the larger cost reduction, designs will either shift to more PV or more batteries. In our example (Fig. 3), the cost optimum point is located on a part of the locus with a low slope; changes in cost will consequently affect the required PV area more than battery storage.

We expect the biggest impact from a change in location to come from the different seasonal variations in available sunlight. Hyderabad is located in the tropics, with moderate seasons and a strong influence from monsoon during the summer months. We expect seasonal variations to affect the optimum average operation time of the load (Fig. 7). Closer to the equator, we anticipate the largest cost savings to shift to longer hours, and vice versa. Consequently, we also expect the presented design approach to be most significant for systems located in the tropics.

4.2. Transfer to other PV-powered systems

Generally, the presented method can be applied to any PV-powered system with accumulable output and flexibility in operation schedule if the time dependent power requirement and the time dependent power availability are known. From these functions, the system can be sized and a first cost optimum point can be calculated (see Fig. 3). Flexible operation can be implemented if the product of the system can be stored for use at a later time. Depending on the temporal properties of the storage, production can be shifted within a certain period (compare Figs. 4 and 5). Load sizing can be achieved by scaling the number of units that generate the product.

For example, the power system of a drip irrigation system could be minimized with optimal sizing of the pumping unit, and flexible operation would allow the power profiles of the electrical load and PV power output to line up. This would reduce the cost of the power system substantially, and could reduce the cost of the system overall. Similarly, a municipal water supply with a water tower supplied by a PV-powered pump could be designed with load sizing and operation flexibility principles to minimize its total cost.

The approach can also be adopted for different systems; in a cooling system, for example, flexible operation can be achieved by either making use of the thermal mass of the location that is cooled and/or by implementing additional thermal storage. Load sizing is achieved by scaling the number of cooling units. Incorporating PV power into these and other similar applications at reasonable cost would accelerate the adoption of PV into new areas.

5. Conclusions

Time-flexible operation and optimal load sizing are applied to better match the power requirement of PV-powered, stand-alone systems to the variable nature of the solar resources. We characterized the cost reductions afforded by time-flexible operation of the load to better match the time-dependent solar irradiance, and by designing the power

characteristics of the load to better suit a variable PV power source. In our approach, we consider a stand-alone system consisting of solar panels, battery storage, and a load that generates some form of accumulable output. We exploit time-flexible operation by selecting the best threshold for turning the output generation on and off, and we adopt load sizing by scaling the load power to obtain the cost-optimum average operating time of the system. The approach uses site-specific weather data to size system components and determine operation protocols, which allows cost reduction for the PV-power system while ensuring persistent operation.

Initially, we considered an idealized reference system with a 1 kW load that generates an unspecified accumulable output for 8 h a day. By relaxing the fixed operating schedule and introducing time-flexible operation, the cost of the exemplary PV-power system (solar panels plus battery) was reduced by 39% from \$2662 to \$1628. Combining time-flexible operation with optimal load sizing allowed for a further cost reduction of 5%, down to \$1503, while maintaining average output generation and daily energy consumption. As flexible operation may require storing surplus output, it is cost-effective if the cost of product storage is below the cost savings afforded by flexible operation—\$1034 for the exemplary system. Flexible operation is, hence, most advantageous if the output can also be used flexibly, or if the need for the generated output coincides with the availability of sun light. This is the case for desalinated water, but also holds for other generated outputs like chilled air or ventilation. Load sizing allows matching the average operating time to the average number of hours during which sunlight is available. Load sizing is most effective if an average daily operating time of 5 to 8 h can be reached. As load sizing requires scaling the load power, it is cost-effective for systems that are intrinsically scalable.

We then reduced our findings to practice by applying the developed approach for the design of PV-powered electrodialysis desalination (EDR) system, designed to generate 10 m³ of drinking water per day in a village near Hyderabad, India. With current technology, the cost of the EDR membranes dominates the overall system costs. In this situation, it is most opportune to operate the system over a long period to minimize the number of membranes needed. As the found optimum operation period of 17:42 h per day greatly exceeds the number of sun hours, the system could not benefit from either time-flexible operation or load sizing. However, when projecting the expected price reduction for EDR membranes at large scale adoption (\$20 instead of the current \$150), the power system becomes the dominant cost factor. In this scenario, the ideal operating time drops to 8:35 h, and time-flexible operation plus load sizing reduces the PV power system cost by 57.6% from \$8935 to \$3788.

Acknowledgements

The authors gratefully acknowledge the funding for the project from Tata Projects Ltd., USAID, the MIT Energy Initiative (MITEI), the MIT Tata Center for Technology and Design, Singapore's National Research Foundation through the Singapore MIT Alliance for Research and Technology's "Low energy electronic systems (LEES) IRG", the National University of Singapore (NUS), and Singapore's National Research Foundation (NRF) through the Singapore Economic Development Board (EDB). Sterling Watson was supported by the MIT Presidential Fellowship.

Appendix A. Supplementary material

Supplementary data associated with this article can be found, in the online version, at <http://dx.doi.org/10.1016/j.solener.2018.01.022>.

References

- Abouzahr, I., Ramakumar, R., 1991. Loss of power supply probability of stand-alone photovoltaic systems: a closed form solution approach. *IEEE Trans. Energy Convers.* 6

- (1), 1–11.
- Beck, T., Kondziella, H., Huard, G., Bruckner, T., 2016. Assessing the influence of the temporal resolution of electrical load and PV generation profiles on self-consumption and sizing of PV-battery systems. *Appl. Energy* 173, 331–342.
- Bermudez, V., 2017. Electricity storage supporting PV competitiveness in a reliable and sustainable electric network. *J. Renewable Sustainable Energy* 9.
- Berney Needleman, D., Poindexter, J.R., Kurchin, R.C., Peters, I.M., Wilson, G., Buonassisi, T., 2016. Economically sustainable scaling of photovoltaics to meet climate targets. *Energy Environ. Sci.* 9, 2122–2129.
- Bian, D., Watson, S., Buonassisi, T., Peters, I.M., Winter, A., 2017. A PV powered EDR System in Chellue, India (submitted for publication).
- Bilton, A.M., Kelley, L.C., 2015. Design of power systems for reverse osmosis desalination in remote communities. *Desalin. Water Treat.* 55, 2868–2883.
- Borowy, B.S., Salameh, Z.M., 1996. Methodology for optimally sizing the combination of a battery bank and PV array in a wind/PV hybrid system. *IEEE Trans. Energy Convers.* 11 (2), 367–375.
- Brihmat, F., Mekhtoub, S., 2014. PV cell temperature/PV power output relationships homer methodology calculation. In: *Conférence Internationale des Energies Renouvelables*.
- Chapman, R.N., 1987. *Sizing Handbook for Stand-Alone Photovoltaic/Storage Systems*. NM: Sandia National Laboratories, Albuquerque.
- Chaurey, A., Kandpal, T.C., 2010. Assessment and evaluation of PV based decentralized rural electrification: an overview. *Renew. Sustain. Energy Rev.* 4 (8), 2266–2278.
- Denholm, P., Margolis, R.M., 2007. Evaluating the limits of solar photovoltaics (PV) in electric power systems utilizing energy storage and other enabling technologies. *Energy Policy* 4424–4433.
- E.e. International Technology Roadmap for Photovoltaic, 2017. “2016 Results”. ITRPV.
- EPRI, 2000. *Century, Water and Sustainability: U.S. Electricity Consumption for Water Supply & Treatment—The Next Half*, Palo Alto, CA.
- General Electric Water & Process Technologies, Westborough, MA, 2014.
- Glavin, M.E., Hurley, W.G., 2012. Optimisation of a photovoltaic battery ultracapacitor hybrid energy storage system. *Sol. Energy* 3009–3020.
- Gowrisankaran, G., Reynolds, S.S., Samano, M., 2016. Intermittency and the value of renewable energy. *J. Polit. Econ.* 124 (4), 1187–1234.
- Guo, S., Wu, C., Danner, M., Nobre, A., Aberle, A.G., Peters, I.M., 2015. Modelling of an integrated standalone streetlamp PV system. In: *42nd IEEE Photovoltaic Specialist Conference (PVSC)*, New Orleans.
- Habib, A.H., Zamani, V., Kleissl, J., 2015. Solar desalination system model for sizing of photovoltaic reverse osmosis (PVRO). In: *ASME 2015 Power Conference*.
- Habib, A.H., Disfani, V.R., Kleissl, J., de Callafon, R.A., 2017. Optimal switchable load sizing and scheduling for standalone renewable energy systems. *Sol. Energy* 144, 707–720.
- Haegel, N.M., Margolis, R., Buonassisi, T., Feldman, D., Frotzheim, A., Garabedian, R., Green, M., Glunz, S., Henning, H.-M., Holder, B., Kaizuka, I., Kroposki, B., Matusbara, K., Niki, S., Sakurai, K., Schindler, R.A., Tumas, W., Weber, E.R., Wilson, G., Woodhouse, M., Kurtz, S., 2017. Terawatt-scale photovoltaics: trajectories and challenges. *Science* 141–143.
- Hangzhou Iontech Environmental Technology Company Limited, Hangzhou, 2014.
- Howell, D., Cunningham, B., Duong, T., Faguy, P., 2016. Overview of the DOE VTO Advanced Battery R&D Program. U.S. Department of Energy, Vehicle Technologies Office.
- F. ISE, 2017. *Photovoltaics Report*. Fraunhofer ISE.
- Jaramillo, L.B., Weidlich, A., 2016. Optimal microgrid scheduling with peak load reduction involving an electrolyzer and flexible loads. *Appl. Energy* 169, 857–865.
- Ji, K., Kim, Y., Choi, K., 2010. Water intake rate among the general Korean population. *Sci. Total Environ.* 408 (4), 734–739.
- Karakaya, E., Sriwannawit, P., 2015. Barriers to the adoption of photovoltaic systems: the state of the art. *Renew. Sustain. Energy Rev.* 49, 60–66.
- Linden, T., Reddy, T.B., 2002. *Handbook of Batteries*, third ed. McGraw-Hill, New York.
- Muhsen, D.H., Ghazali, A.B., Khatib, T., 2016. Multiobjective differential evolution algorithm-based sizing of a standalone photovoltaic water pumping system. *Energy Convers. Manage.* 118, 32–43.
- Nikolaidis, A.I., Koumparou, Y., Makrides, G., Efthymiou, V., Georgiou, G.E., Charalambous, C.A., 2016. Reliable integration of a concentrating solar power plant in a small isolated system through an appropriately sized battery energy storage system. *IET Renew. Power Gener.* 10 (5), 735–742.
- Nykvist, B., Nilsson, M., 2015. Rapidly falling costs of battery packs for electric vehicles. *Nat. Clim. Change* 5, 329–332.
- Olcan, C., 2015. Multi-objective analytical model for optimal sizing of stand-alone photovoltaic water pumping systems. *Energy Convers. Manage.* 100, 358–369.
- Pearsall, N. (Ed.), 2017. *The Performance of Photovoltaic (PV) Systems: Modelling, Measurement and Assessment*, vol. 1 Woodhead Publishing.
- Available: pvinsights.com (accessed 1 June 2017).
- National Renewable Energy Laboratory (NREL), 2016. *NSRDB Data Viewer*. Available: < <https://maps.nrel.gov/nsrdb-viewer/> > (accessed 16 September 2016).
- Sahraei, N., Watson, S.M., Pennes, A., Peters, I.M., Buonassisi, T., 2017. Design approach for solar cell and battery of a persistent solar powered GPS tracker. *Jpn. J. Appl. Phys.* 56 (8S2).
- Shrikhande, N.S., 2016. Bengaluru.
- Suniva Optimus Series Monocrystalline Solar Modules, 2016. < <https://www.wholesalesolar.com/cms/suniva-suniva-opt330-72-4-100-silver-mono-solar-panel-specs-1610309543.pdf> > (accessed 20 May 2016).